Pure & Appl. Chem., Vol. 62, No. 9, pp. 1761–1772, 1990.
Printed in Great Britain.

Metallurgy of open-bath plasma processes

Nicholas A. Barcza, Thomas R. Curr, and Rodney T. Jones

Mintek, Private Bag X3015, Randburg 2125, South Africa

Abstract - Thermodynamic simulation of the carbothermic chemical reactions likely to occur in the open bath of a d.c. transferred plasma-arc furnace using a standard slag comprising CaO, MgO, Al_2O_3, and SiO_2 as a basis, and with FeO, Cr_2O_3, MnO, and ZnO added at various carbon levels, has shown that the high temperatures expected in the arc attachment zone (AAZ) can cause unacceptable products to be produced at the expense of the desired ones and result in higher consumption of energy. The thermal inertia of the AAZ can be used in efforts to assess the level of control needed over the feed rate, distribution of the feed, and power input of a particular process in order to limit high temperature excursions, which cause so-called 'side reactions', e.g. the reduction of MgO to Mg vapour.

INTRODUCTION

A number of novel pyrometallurgical processes have been successfully demonstrated, some of which are currently being commercially exploited. These processes use an open bath of molten slag and metal into which the materials to be treated are fed, and onto which a transferred plasma-arc column is directed to effect the input of intense thermal energy. The energy is required to maintain the bath in a liquid state and to drive the chemical reactions, which are normally endothermic, thereby producing the desired products. Successful applications include the remelting and smelting of ferrochromium from alloy fines and chromite-ore fines respectively (ref.1), the remelting of ferromanganese fines (ref.2), the production of magnesium by a thermal process (ref.3), and the fuming of zinc metal from waste materials, i.e. dust and slags (ref.4).

The open-bath transferred plasma-arc furnace offers significant advantages over submerged-arc furnaces, or furnaces that have a solid layer of burden above the molten bath, for certain processes, including the following. Fine materials can be fed direct (i.e. without agglomeration) to the furnace, and the feed and power inputs can be controlled independently. Hence, it is possible to choose the overall temperature at which the process is operated. Also, high feed and power fluxes are attainable, which results in high productivity from a relatively small furnace volume, the process metallurgy is flexible, and products meeting the required specifications are attainable, even from low-grade raw materials in some instances.

The potential disadvantages of the open-bath configuration include the following. There is a high specific loss of energy via radiation from the exposed surface of the bath and the plasma-arc column, and via the sensible energy in the high-temperature off-gas; certain vapour species that would otherwise be largely captured in the solid burden of a submerged-arc furnace are lost, and careful design of the refractory lining is necessary to ensure long life. A critical requirement is the need for continuous balancing of the feed and power inputs, particularly in the arc attachment zone (AAZ), to minimize unwanted side reactions (i.e. reactions other than those intended).

A detailed examination of the chemical and physical properties of the chemical species associated with a number of pyrometallurgical processes was recently carried out using Mintek's Pyrosim computer program (ref.5). This was done in an effort to identify what process chemistry, (i.e. reactions) would take place under the potentially wide range of operating conditions that could be found in an open-bath transferred plasma-arc furnace. A better understanding of that subject should result in improved operation of processes which are already being operated successfully, and could extend the application of open-bath transferred plasma-arc technology to processes that have not yet been satisfactorily proven, e.g. the smelting of ferromanganese alloys.

MASS AND ENERGY BALANCES IN PYROMETALLURGICAL PROCESSES

Since the feed rate of the materials and the input of power via the thermal plasma arc are independent, a very careful balance must be reached so that the most appropriate temperature distribution across the bath can be attained and maintained. Careful consideration must be given to the identification of suitable criteria relating to mass and energy balances, so that the conditions leading to unwanted side reactions can be minimized. Such reactions demand additional energy, and result in the production of undesirable reaction products.

The predicted theoretical energy requirement for a given process under steady-state conditions can be calculated from thermodynamic considerations. The chemical constituents in the feed and those expected in the products must be specified, as must the process temperatures and pressure. The required feed rate to the process can be determined by calculation of the effective power available to the process after the 'heat losses', i.e. the rate at which energy is lost from the furnace have been accounted for. These losses occur essentially through the shell of the furnace (the hearth, roof, and side walls) and in any water-cooled components inside or on the furnace. The energy losses in the off-gas are normally specified in the thermodynamic considerations of the process.

Under steady-state conditions, a balance between feed rate and power input can be achieved relatively straightforwardly based on theoretical calculations and empirical operating experience (in particular for the determination of the actual energy losses and the analytical composition of the products). During more-dynamic operating conditions, i.e. during heating or cooling of the furnace, changing of the recipe or a component of the feed, setting of a different power level to yield a greater or smaller throughput, or restarting of the furnace after a shut-down, optimum control of the process chemistry is often extremely difficult.

Fig. 1 shows the relationship between the selected power level and the feed rate, which is a function of the required specific energy consumption, expressed in kilowatt-hours per kilogram of feed (or product).

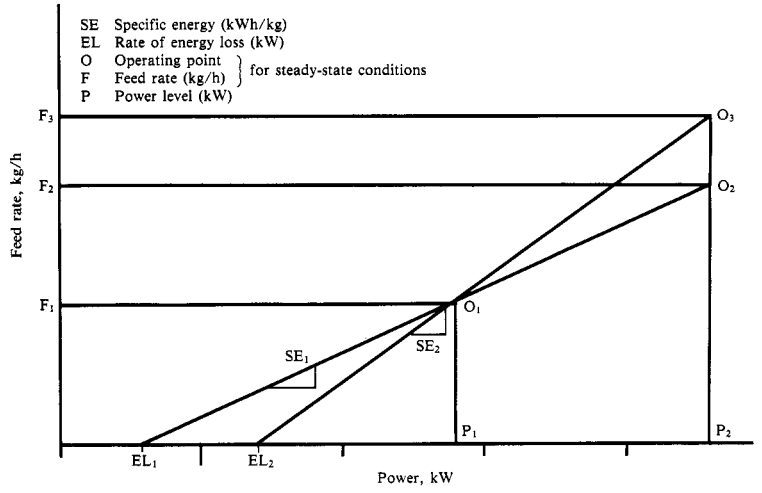

Fig. 1. The relationship between feed rate and power level at different rates of energy loss and specific energy consumption

It is very important to distinguish clearly between the specific energy (SE) requirement (kWh/kg) and the rate of energy loss (EL) (kW). An operating point O_1 with a feed rate F_1 for steady-state conditions can be reached, given an apparent value for the rate of energy loss, say EL_1, and a specific energy requirement SE_1 at a power level of P_1(kW). If the power level is increased to, say P_2(kW), based on the values EL_1 and SE_1, then operating point O_2 should be used for the setting of the feed rate F_2. However, if the values of EL_1 and SE_1 were incorrect (i.e. if they merely compensated for each other at point O_1, as can often occur in practice), and the true values were EL_2 and SE_2, operating point O_3, which is about 25 per cent higher in terms of feed rate F_3 than is F_2, should have been selected. As a result of this error, overheating of the furnace would occur, starting with the AAZ, and moving progressively to the side walls and hearth.

If the thermocouples in the side wall are used as the only monitors of the process (i.e. the bath temperature), it could take several hours for the imbalance between feed and power to be detected. However, the temperature in the AAZ, would be expected to increase substantially in a much shorter time, typically minutes rather than hours. The increased energy input would be used as follows. Some energy would be transferred away from the AAZ to the surroundings, some would be consumed in the AAZ itself (driving unwanted side reactions), while the balance would result in the establishment of a new, higher temperature level.

Modelling of the energy transfer from the AAZ into the surrounding zones is extremely complex, but Brent has, on behalf of Mintek, made considerable progress in this area of research while studying at the University of Minnesota (ref.6). The temperature profiles within a liquid bath can now be calculated, using Brent's model, as a function of the power input and furnace geometry, but only in the absence of chemical reactions.

Even under steady-state conditions, the temperature distribution on the surface of the bath is expected to exhibit a steep gradient from the central arc attachment zone (probably 2000 to 3000°C) to the side walls (normally 1000 to 1500°C) as a result of the very high temperatures present in the plasma column (10 000 - 20 000 K). The choice of the recipe and the distribution of the feed between the AAZ and the area towards the side walls can assist in the control of the bath temperature and, hence, the reactions. However, the chemical reactions occurring in the AAZ are largely dominated by the high temperatures in that region and in the plasma-arc column.

THREE-ZONE BATH MODEL

The contents of an open-bath transferred plasma-arc furnace can be divided into three zones, namely: the arc attachment zone (AAZ), the liquid bath zone outside the AAZ, and the freeze-lining zone (which could be the refractory lining of the furnace or solid material associated with the process itself, e.g. slag, metal, or components in the feed that could be partly reacted). The zones are illustrated in Fig. 2.

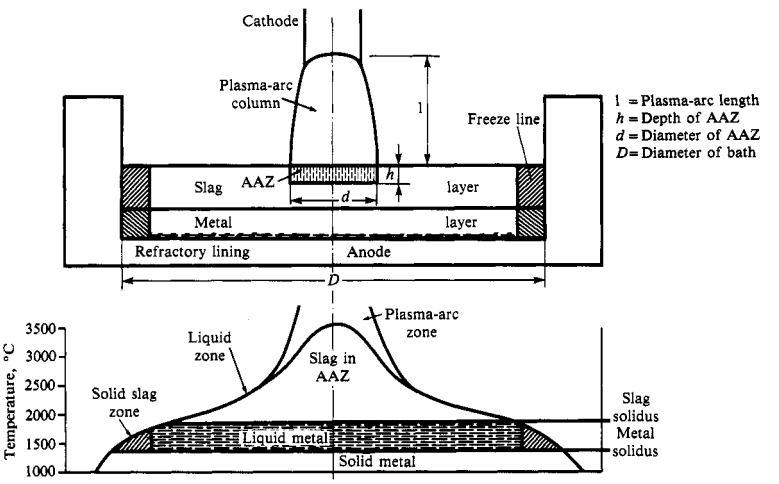

Fig. 2. The three zones of an open-bath transferred plasma-arc furnace shown schematically in elevation

The scale-up of open-bath plasma furnaces from the 0.1 MW laboratory scale to the 1 MW pilot-plant scale and up to the 20 MW industrial scale is associated with a moderate increase in the power flux and power-to-mass ratio in the AAZ, as shown in Fig. 3. However, the projected scale-up to 60 and 100 MW would result in significantly higher values of power flux and power-to-mass ratio. The implications of this effect on the requirements for control of the balance between feed rate and power input were therefore studied.

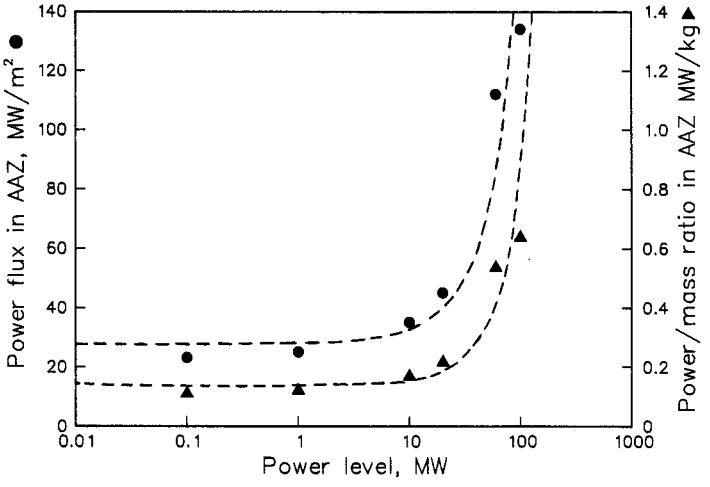

Fig. 3. The relationship between the power flux and power-to-mass ratio in the AAZ, and the power level as a function of scale-up

SIMULATION OF THE PROCESS CHEMISTRY IN THE AAZ OF THE PLASMA FURNACE

The slag system $CaO\text{-}MgO\text{-}Al_2O_3\text{-}SiO_2$ was chosen for the process simulations. Equal proportions of 25 per cent by mass of these four oxides were used to produce a slag with an acceptable liquidus temperature and with acceptable physical-chemical properties (such as viscosity and electrical conductivity). Reducible oxides such as iron oxide (FeO), chromium oxide (Cr_2O_3), manganese oxide (MnO), and zinc oxide (ZnO), were introduced into the slag phase. The size of the addition was 10 per cent by mass (e.g. 100 kg of slag plus 10 kg of FeO). The carbothermic reduction reactions were simulated under equilibrium conditions from 1600 to 2600°C, using Mintek's Pyrosim computer program and available thermodynamic data (extrapolated where necessary). In some instances, 1400°C was used as the lowest temperature.

The systems were modelled assuming multicomponent multiphase chemical equilibrium between the gas, slag, and metal phases. The possible formation of a solid carbide phase was also taken into account. The equilibrium calculations were performed using the technique of free-energy minimization. The non-idealities in the slag and metal phases were handled using the 'Ideal Mixing of Complex Components' approach (ref.7).

The lower temperature of 1600°C (or 1400°C) was chosen to represent the normal operating temperature for a slag of the above-mentioned composition, thus ensuring its fluidity and the dissolution and reduction of the added oxides of iron, chromium, manganese, and zinc by carbon. The upper temperature of 2600°C was chosen as being representative of the temperature levels that, it was expected, would be attained in the AAZ under operating conditions where some degree of overpowering was taking place.

The carbon additions were varied between 1 and 15 per cent by mass (relative to the four-component slag) to represent the extremes of mildly - and strongly reducing conditions (i.e. where the amount of carbon in excess of the stoichiometric amount required to completely reduce the oxide added to the slag was varied from 60 to over 500 per cent).

Tables 1 to 4 present some of the results from the simulations of the process chemistry in the AAZ. Table 1 shows the distribution of magnesium and silicon to the vapour phase in the four-component slag system alone, while Tables 2 to 4 show the distributions obtained from the systems in which FeO was added to the slag together with Cr_2O_3, MnO, and ZnO. The carbon additions shown are relative to the four-component slag only. An example of an extract from the detailed data base used for plotting of the graphical relationships is shown in Table 5.

TABLE 1. The distribution of magnesium and silicon to the vapour phase as a percentage of their contents in the feed

Temperature °C	Carbon addition					
	2%		5%		10%	
	Mg_v	Si_v	Mg_v	Si_v	Mg_v	Si_v
1600	0	0	0	0	0	0
1800	1	0	4	1	8	1
2000	20	10	49	27	85	50
2200	20	10	49	27	90	63
2400	20	10	49	27	89	63
2600	21	9	49	26	89	63

v Vapour phase

TABLE 2. The distribution of magnesium, silicon, iron, and chromium to the metal, slag, and vapour phases as a percentage of their contents in the feed

Temperature °C	Carbon addition														
	2%					5%					10%				
	Mg_v	Si_v	Fe_m	Cr_s	Cr_m	Mg_v	Si_v	Fe_m	Cr_s	Cr_m	Mg_v	Si_v	Fe_m	Cr_s	Cr_m
1600	0	0	91	84	16	0	0	99	0	100	0	0	100	0	100
1800	0	0	87	79	21	0	0	99	0	100	16	1	100	0	100
2000	0	0	80	74	26	3	1	98	1	99	34	8	100	0	100
2200	1	1	71	70	30	9	4	94	6	94	48	21	99	0	100
2400	4	2	57	72	28	19	10	82	29	71	57	32	94	4	96
2600	14	8	25	90	10	34	20	49	72	28	66	41	77	31	69

m Metal phase
s Slag phase
v Vapour phase

TABLE 3. The distribution of magnesium, silicon, iron, and manganese to the metal and vapour phases as a percentage of their contents in the feed

Temperature °C	Carbon addition														
	2%					5%					10%				
	Mg_v	Si_v	Fe_m	Mn_v	Mn_m	Mg_v	Si_v	Fe_m	Mn_v	Mn_m	Mg_v	Si_v	Fe_m	Mn_v	Mn_m
1400	0	0	99	0	3	0	0	99	0	6	0	0	99	0	6
1600	0	0	98	1	7	0	0	100	4	61	0	0	100	4	61
1800	0	0	95	3	10	2	0	100	23	49	20	1	100	33	63
2000	1	0	90	8	8	9	3	99	51	21	45	11	100	76	19
2200	2	1	78	17	5	18	7	94	64	7	57	26	99	89	4
2400	7	3	49	29	2	26	12	73	66	2	65	36	90	90	2
2600	14	7	0	37	0	37	19	11	68	0	71	43	60	90	1

m Metal phase
v Vapour phase

TABLE 4. The distribution of magnesium, silicon, iron, and zinc* to the metal and vapour phases as a percentage of their contents in the feed

Temperature °C	Carbon addition								
	2%			5%			10%		
	Mg_v	Si_v	Fe_m	Mg_v	Si_v	Fe_m	Mg_v	Si_v	Fe_m
1600	0	0	33	0	0	100	0	0	100
1800	0	0	32	2	0	100	37	4	100
2000	0	0	31	8	3	99	47	12	100
2200	5	3	0	16	7	93	58	26	99
2400	5	3	0	24	11	68	65	37	90
2600	6	3	0	35	19	0	71	43	61

* 100 per cent zinc in vapour in all instances
m Metal phase
v Vapour phase

TABLE 5. Example of detailed data for a single temperature and level of carbon addition

System: 100 kg of four-component slag & 10 kg of FeO & 10 kg of C
Temperature: 2000°C
Energy required: 173 kWh
Masses of phases at equilibrium (kg)
Gas: 35.02 Slag: 73.48 Metal: 11.50

v Vapour phase
s Slag phase
m Metal phase

Phase composition (mass %)							
Slag					Metal		
FeO	SiO_2	CaO	MgO	Al_2O_3	Fe	Si	C
0	18.2	33.9	14.0	33.9	67.6	32.0	0.004

Distribution of elements between phases (%)								
Si_v	Si_s	Si_m	Ca_v	Ca_s	Ca_m	Mg_v	Mg_s	Mg_m
15.1	53.4	31.5	0.35	99.6	0.024	58.8	41.2	0.000546
Al_v	Al_s	Al_m	Fe_s	Fe_m	C_v	C_m		
0	99.70	0.30	0.30	99.97	99.995	0.004		

RESULTS OF THE SIMULATIONS OF THE AAZ

On heating of the four-component slag, $CaO-MgO-Al_2O_3-SiO_2$, from 1600 to 2600°C in the absence of carbon, very little chemical change will take place. However, as carbon is progressively introduced into the system, both MgO and SiO_2 are reduced. An FeO addition of 10 per cent by mass to the system has only a relatively minor influence on the reduction of MgO and SiO_2. The results for the simulations in the slag system with FeO are shown in Figs. 4 and 5 for magnesium and silicon respectively.

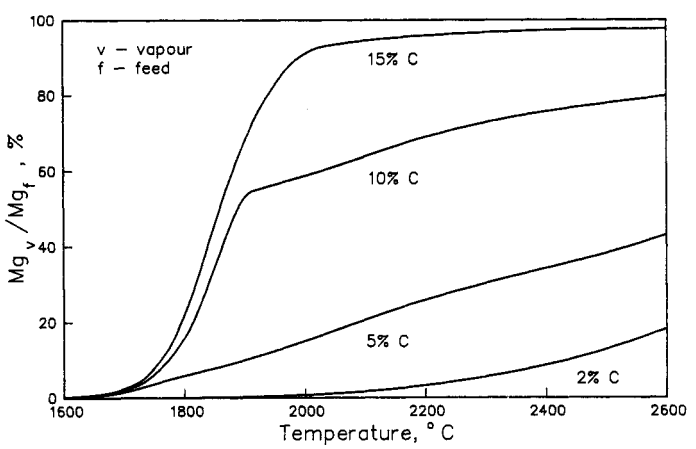

Fig. 4. The proportion of magnesium in the feed reporting to the vapour phase as a function of temperature and carbon addition for the system with 10 per cent FeO added

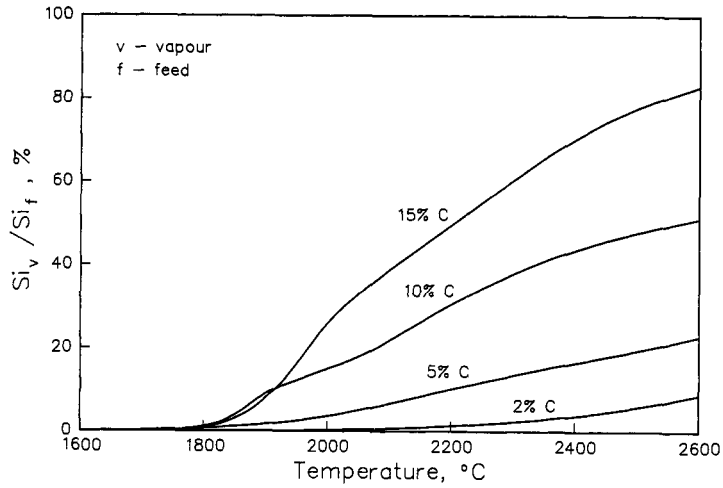

Fig. 5. The proportion of silicon in the feed reporting to the vapour phase as a function of temperature and carbon addition for the system with 10 per cent FeO added

The proportions of magnesium (as Mg vapour) and silicon (as SiO vapour) relative to their respective contents in the feed are shown as functions of temperature and carbon addition in these two figures. It is interesting to note that the relative proportion of magnesium is greater than that of silicon at all similar temperature levels and for similar carbon values. For example, at 2000°C and 10 per cent carbon, the Mg_v/Mg_f ratio is about 60 per cent, whereas the Si_v/Si_f ratio is only 15 per cent. Fig. 5 shows that, at about 1900°C the Si_v/Si_f ratio for the addition of 15 per cent carbon is less than that for 10 per cent carbon. This is because, at the higher carbon level, silicon carbide forms more readily than does silicon monoxide. Fig. 6 shows the considerable increase in energy consumption with increased temperature and carbon addition to the standard slag phase to which FeO (10 per cent by mass) has been added. Operation of the process at 1600°C requires about 50 to 70 kWh per 110 kg of feed (plus the carbon addition) and there is only a minor increase with carbon addition from 2 to 15 per cent in this range (50 to 70 kWh). At 2000°C, the energy requirement increases from about 75 to 240 kWh per 110 kg of feed (plus carbon) as the carbon addition is raised from 2 to 15 per cent by mass. At 2600°C, the value for a carbon addition of 2 per cent is 125 kWh and, for one of 15 per cent, it is 305 kWh per 110 kg of feed (plus carbon).

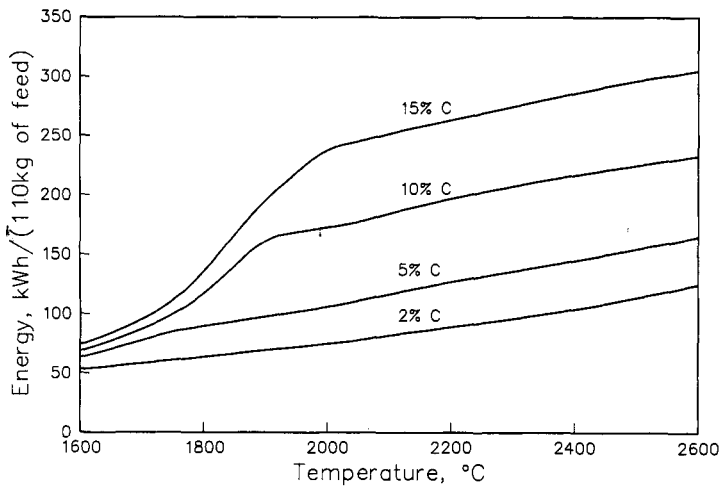

Fig. 6. The calculated energy consumption as a function of the process temperature and carbon addition for the standard slag with 10 per cent FeO

Fig. 7 shows a rather surprising phenomenon, namely that the reduction of MgO is more favourable than that of FeO at temperatures higher than about 2400°C, particularly where the carbon addition exceeds 5 per cent. The iron distribution to the metal falls to less than 40 per cent, and the proportion of magnesium reporting to the vapour phase increases to almost 80 per cent at 2600°C.

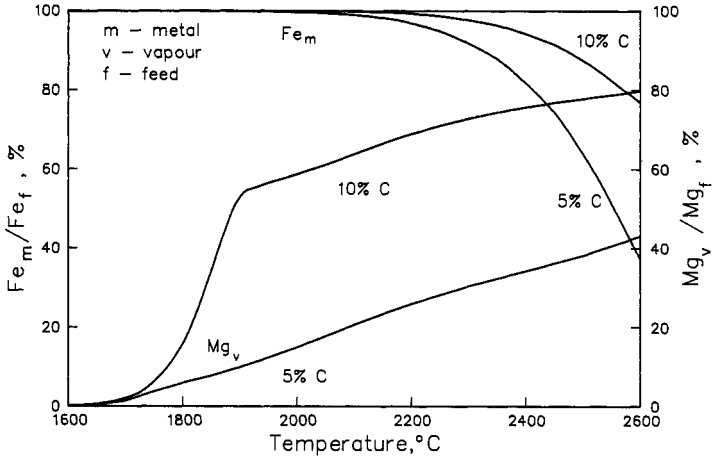

Fig. 7. The proportion of iron and magnesium reporting to the metal and vapour phases respectively as a function of temperature at carbon additions of 5 and 10 per cent

The results when Cr_2O_3 and FeO (each at 10 per cent by mass), are present in the standard slag are similar to those when FeO is present alone. At low carbon additions and lower temperatures, the iron is selectively reduced into the metallic phase, as shown in Table 3. At more elevated temperatures and higher carbon additions, the tendency for magnesium oxide to be reduced and to vaporise as magnesium metal and for silicon monoxide gas to form increases to levels similar to those shown in Figs. 4 and 5.

At carbon levels of less than 5 per cent, the reduction of chromium to the metallic phase is more favourable at 1800°C than it is at 1600°C. Iron oxide is optimally reduced at about 1600°C and about 4 per cent carbon, as shown in Fig. 8. At 2600°C, the reduction of both iron and chromium oxides is less favourable than at the lower temperatures as a result of the preferred reduction of MgO and SiO_2.

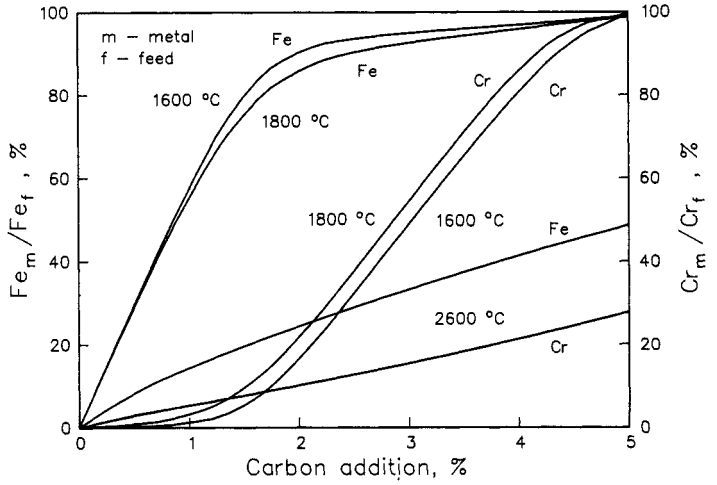

Fig. 8. The distribution of iron and chromium to the metal phase as a function of carbon addition at 1600, 1800, and 2600°C

Manganese oxide is reduced carbothermically to manganese metal, which has a relatively low boiling point (about 2060°C) and a high vapour pressure. The manganese is therefore readily distributed to the vapour phase, as can be seen in Fig. 9, where the manganese distribution is shown as a function of temperature for a carbon addition of 5 per cent. The optimum recovery of manganese from the slag into the metal phase (approximately 60 per cent under these conditions) is achieved at about 1600°C, where the vapour losses are still less than 5 per cent of the manganese in the feed.

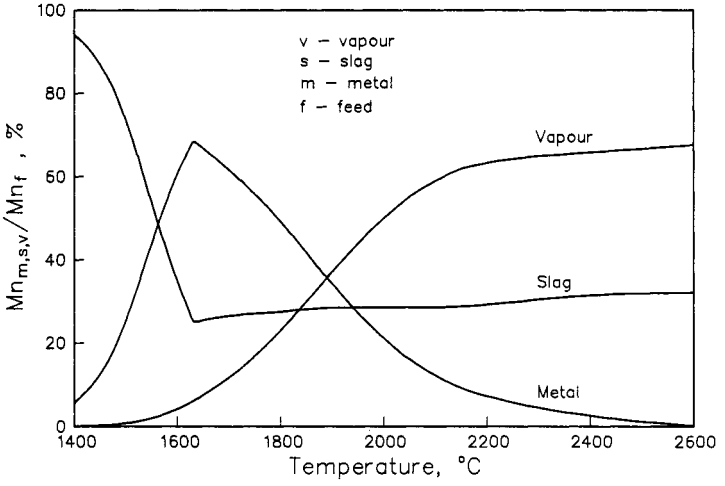

Fig. 9. The distribution of manganese between the vapour, slag, and metal phases as a function of temperature for a carbon addition of 5 per cent

THE THERMAL INERTIA MODEL AND CONTROL OF THE PROCESS

Steady-state conditions should be maintained in the AAZ at the optimum temperature level to maximize the required chemical reactions, give high recoveries of the products, and minimize the undesirable side reactions. A general thermal inertia model (TIM) has been developed for use in evaluation of the control requirements of the pyrometallurgical processes discussed earlier. The resistance to a change in temperature, which has been termed 'thermal inertia', can take several forms, e.g. heating of the slag and metal, shifting of the equilibrium between the metal and slag phases, driving of the side reactions, and increase of the molten-bath area. In the present work, the time taken for the temperature of the AAZ to rise by 100°C was used as a measure of thermal inertia. Although the thermal inertia of the bath as a whole is of importance in regard to the furnace reaching a given steady-state condition, it is the AAZ that is of primary concern when control of the process itself is borne in mind.

The sensitivity required in the control of the balance between feed rate and power input can be determined by use of the thermal inertia model. When the temperature of the slag phase is raised on its own from, say 1600 to 1700°C, there is relatively little thermal inertia. Fig. 10 shows that the time required for the AAZ to reach a higher temperature decreases markedly with increased overpowering of the process. An example of the time taken to reach 400°C higher is also shown in this diagram. Hence, the estimated 0.93 kg of slag (see Table 6) in the AAZ (of the total of 100kg of feed) can be heated by 100°C in only about 6 minutes if the power exceeds that required for steady-state conditions by only 1 per cent. When FeO (10 per cent by mass) is added to the slag, the time taken for the AAZ to reach 1700°C from 1600°C is about 16 minutes, i.e. about three times longer.

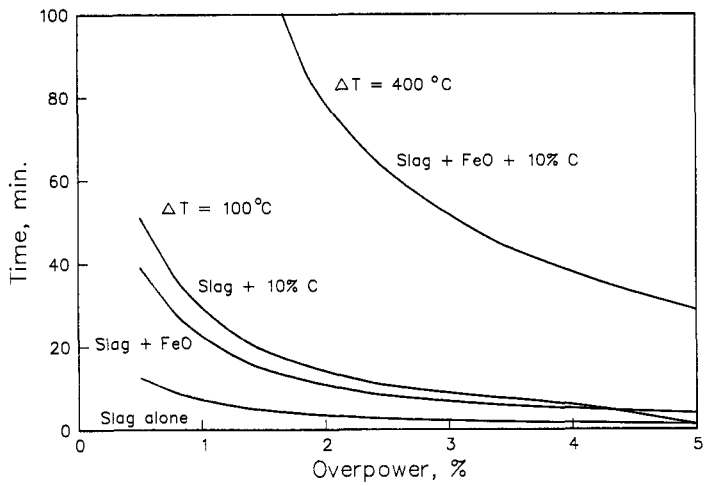

Fig. 10. The time taken for the AAZ to rise by 100°C and 400°C as a function of the overpowering of the furnace

Fig. 11 shows the increase in thermal inertia in the AAZ a function of temperature for the slag and the slag plus 10 per cent carbon at 2 and 5 per cent overpowering.

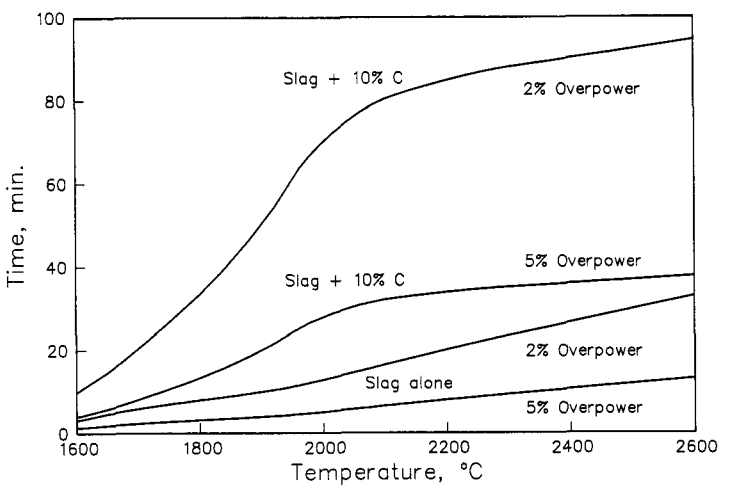

Fig. 11. Thermal inertia as a function of temperature and carbon addition

The uncertainties regarding the calculation of the true thermal inertia in the AAZ result from the difficulties encountered in measurement of the area of the AAZ and, more particularly, the depth to which the high temperature of the plasma arc penetrates the molten bath. Modelling of the transfer of thermal energy by radiation, convection, and conduction from the surface of the AAZ to the surrounding areas, in the furnace atmosphere and the liquid bath is very complex. If, as postulated by Brent (ref. 6), the depth to which the AAZ penetrates beneath the slag (shown as h in Fig. 2) is relatively shallow and the diameter of the AAZ (shown as d in Fig. 2) is only slightly greater than that of the electrode (about 50 per cent greater), then the volume and, hence, the mass of the AAZ is rather small compared to that of the total bath.

Examples of furnaces on the 200 kW pilot-plant scale, 10 and 20 MW industrial scale, and 60 and 100 MW projected scales were investigated with regard to the thermal inertia in the AAZ and the furnace bath as a whole. The slag system with an FeO content of 10 per cent was used. Small pilot-plant plasma-arc furnaces can be used to simulate larger furnaces in many respects, if considerations such as power flux are at a similar level. With scale-up from 200 kW, the energy-loss term in the energy balance is expected to decrease considerably as a percentage of the power level from about 25 per cent (i.e. 50 kW) at the 200 kW level to about 15 per cent (i.e. 3 MW) at 20 MW to less than 10 per cent (i.e. less than 10 MW) at 100 MW.

The size of the AAZ (i.e. area/volume) becomes progressively a smaller proportion of the total furnace volume, and the ratio of the size of the AAZ to the power level also decreases. This results in greater sensitivity to the balance between feed and power, in that the absolute rates are not only much greater, but the thermal inertia in the relatively smaller proportional AAZ volume is lower, as shown in Table 6. Therefore, at even 0.5 per cent overpower at 100 MW, it would take the projected mass of 157 kg of slag in the AAZ just under 4 minutes to reach 1700°C.

TABLE 6. Power flux in the AAZ as a function of scale-up to various projected power levels

Power level MW	Current kA	Voltage V	Arc length mm	Electrode diameter mm	Diameter of AAZ * mm	Area of AAZ m^2	Power flux MW/m^2	Mass in AAZ kg	Time to 100°C above 1600°C min **
0.1	1	100	50	50	75	0.0044	23	0.93	21
1	4	250	125	150	225	0.0398	25	8.36	19
10	25	400	200	400	600	0.283	35	59.4	14
20	40	500	250	500	750	0.442	45	92.8	11
60	100	600	300	550	825	0.535	112	112.0	4.3
100	130	700	350	650	975	0.747	134	157.0	3.7

* Diameter of AAZ assumed to be 1.5 x electrode diameter
** At 0.5 per cent overpower

SUMMARY AND CONCLUSIONS

(1) The control over the feed rate and power level to within about 0.5 per cent accuracy appears to be necessary, particularly at power levels greater than 20 MW, so that the unwanted increase in energy consumption caused by increased bath temperature and the favouring of undesirable side reactions can be avoided.

(2) These side reactions include the carbothermic reduction of magnesium oxide to magnesium vapour and of silicon dioxide to silicon monoxide gas. Temperatures above 2000°C and carbon additions of 5 per cent and higher favour the reduction of these two common slag-forming oxides even, somewhat surprisingly, in preference to that of iron oxide.

(3) There is a marked increase in the thermal inertia of the AAZ and furnace bath as a whole with increased temperature and level of carbon additions as more endothermic reactions occur. This thermal inertia tends to limit to some extent a temperature runaway in the AAZ under equilibrium conditions. However, in an open system, in which vapour species can be transported away from the bath (as would occur in practice), rapid deviations from optimum operation can easily occur.

(4) Direction of the feed materials into the AAZ generally has a beneficial effect, because it controls the temperature and chemical reactions taking place. The carbon content of the recipe in this zone can play a major role in determining what reactions take place. To limit and control side reactions, the carbon level can be set to below the stoichiometric level for complete reduction in this high-temperature zone (above 2000°C). The balance of the carbon needed to complete reduction of the required product can be added to the slag bath away from the AAZ in the lower-temperature region (say 1600°C) under conditions much less conducive to the development of side reactions.

(5) It has been shown both theoretically and in practice that iron and chromium ore can be successfully smelted in an open-bath plasma furnace under the appropriate operating conditions. The smelting of manganese ore is predicted to be much more difficult because of the potential for extensive losses of manganese to the vapour phase. However, it should be possible to smelt manganese ore successfully with limited carbon in the feed to the AAZ, the balance (and probably some excess) of the carbon being fed to the lower-temperature (below 1600°C) region outside the AAZ.

(6) The thermodynamic determination of the process chemistry of the species associated with a particular process under the temperature conditions likely to be present allows the optimum feed recipe, feed locations, process control, and equipment to be designed. The suitability of an open-bath transferred plasma-arc furnace for several metallurgical processes has been investigated on this basis with some rather unexpected results.

(7) If this thermodynamic approach were to be combined with the dynamics of the system, i.e. if the mass and energy transfer rates between the zones of the bath and the furnace environment were to be included, as well as the rate of the chemical reactions under open conditions (i.e. not a closed equilibrium), an even better assessment of the thermal inertia and control requirements should be possible. The present investigation has nevertheless demonstrated the value of this approach, which has not only allowed the metallurgical reactions and energy-balance considerations in an open-bath plasma furnace to be evaluated for several processes, but which could be extended to other processes.

Acknowledgement

This paper is published by permission of Mintek. Thanks are also due to Mr P.L. van der Merwe for carrying out many of the simulations and to Dr A.D. Brent for the technical information on the numerical modelling of heat transfer and fluid flow in the hearth of a d.c. transferred plasma-arc furnace.

REFERENCES

1. Anon., *S. Afr. Mech. Eng.* 39, 197-229 (1989).

2. N.A. Barcza, *J. S. Afr. Inst. Min. and Met.* 1, 317-333 (1986).

3. A.F.S. Schoukens, Preprint, Extraction Metallurgy '89, London, Institution of Mining and Metallurgy (1989).

4. P.M. Cowx and B. Roddis, *Reinhardt Schumann International Symposium on Innovative Technology and Reactor Design in Extraction Metallurgy,* Colorado Springs, The Metal Society of AIME, 73-85 (1986).

5. R.T. Jones, *Proceedings, APCOM 87,* Johannesburg, South African Institute of Mining and Metallurgy, vol.2, 265-279 (1987).

6. A.D. Brent, University of Minnesota, Private communication (1989).

7. R.T. Jones and B.D. Botes, Proceedings, *Colloquium on Ferrous Pyrometallurgy*, Vanderbijlpark, South African Institute of Mining and Metallurgy. (1989).